Available online www.jsaer.com

***Journal of Scientific and Engineering Research*, 2018, 5(9):327-337**

Research Article

ISSN: 2394-2630
CODEN(USA): JSERBR

Acoustic Impedance Attribute for Lithology Discrimination in HEK-Field of Niger Delta Basin of Nigeria

Opiriyabo I. Horsfall*, Cliff-Ekubo W. C.

Department of Physics, Rivers State University, Port Harcourt, Nigeria

Abstract This paper presents acoustic impedance determination for lithology discrimination in part of Niger Delta basin of Nigeria using suits of composite well Logs namely HEK-1, HEK-2, HEK-3, and HEK-4 in the same location in the Niger Delta. Sonic log and density log were used to delineate the travel times, acoustic velocities, densities, and acoustic impedances at various depth. Cross plots of depth against velocity, depth against density, and depth against acoustic impedance were computed. Acoustic impedance was used to discriminate the different lithologies. The results showed that velocity, density, and acoustic impedance all increased with depth. The resulting lithologies as discriminated in the four wells using the acoustic impedance indicator is shale and sandstone with values ranging between 3002135Kg/m^{2}s and 14049297Kg/m^{2}s.

Keywords Acoustic Impedance, Lithology, Shale, Sandstone

Introduction

Acoustic Impedance (Z) is a basic physical property of rocks. It describes how much resistance an elastic wave encounters as it propagates through the rock. Acoustic impedance depends on the density of the rock and the velocity of the elastic wave. Lithology describes the solid (matrix) portion of the rock, generally in the context of the description of the primary mineralogy of the rock [1]. Different lithologies have different mineralogical compositions and particle sizes based on the source materials, and depositional environments, which influences the temperature and velocity of such formations [2-4]. The lithological features of rocks such as texture, size, shape, colour, streak, specific gravity, lustre, tenacity, density etc, are basically influenced by the mineralogical content of the rocks [5]. The discrimination of a bed's lithology is fundamental to all reservoir characterization because the physical and chemical properties of the rock that holds hydrocarbons and/or water affect the response of every tool used to measure formation properties. Understanding reservoir lithology is the foundation from which all other petrophysical calculations are made. To make accurate petrophysical calculations of porosity, water saturation, and permeability, the various lithologies of the reservoir interval must be discriminated and their implications understood [6]. In Geophysics, Acoustic impedance which is a basic physical property of rocks is the product of acoustic velocity (V) and density (ρ). Acoustic velocity is a geophysical parameter that measures the rate of change of displacement as sound wave is propagated through the stratified geology of an area from the source to receiver [3] cited in [7].

The Velocity and density of the formation are gotten from well log, which is the record of the measurements of the physical properties of surrounding rocks with a sensor located in a borehole as a function of depth [8]. This information is then used to derive the velocity of elastic waves through the formation. The density is derived from density log which measures the density of the formation. Well data reveal about the geological structures and the lithologies of the subsurface. Well lithology analysis aims at estimating lithological and reservoir properties from logs characteristics [5]. [9] researched on Estimation of Shear Wave Velocity for Lithological Variation in the North-Western Part of the Niger Delta Basin of Nigeria. In order to achieve the aim of their

study Gamma ray log was used for the lithological differentiation. Sonic log was used for computation of compressional wave velocity. Shear wave velocity was determined from compressional wave velocity. The analysis of shear and compressional wave velocity showed a general conventional trend of increase in velocity with depth but varies at some depth due to lithological variation, heterogeneity and anisotropic nature of the earth. Poisson's ratio (V_p/V_s) is greater in shaly formation than in sandy formations. [5] in their work,

Estimation of lithological and mineralogical contents of rocks from Matrix density in parts of Niger Delta Basin Nigeria, using Well-log Data affirmed the already established lithologic sequence of the Niger Delta basin, which is majorly composed of sandstone and shale with mineralogical components of quartz and clay minerals respectively. Also, they showed that shale is denser than sandstone. [1] applied the method of Cross plotting of Rock Properties for Fluid and Lithology Discrimination in a Niger Delta Oil Field using well log data. Well data for six suits of wells were used; Wells -02 and well-06 having more well logs were used in the analysis. The reservoir was evaluated using gamma ray logs, volume of shale, resistivity and neutron porosity. Sand lithology showed low gamma ray, high resistivity and low acoustic impedance. Cross plotting was carried out and the plots with most outstanding results were V_p/V_s ratio against Acoustic impedance which distinguished the REV-01 reservoir into hydrocarbon zone, brine zone and shale zone. Second, lambda rho (incompressibility) against V_p/V_s discriminated the reservoir of interest in sands and shale/sand/shale sequences.

Location and Geology of the Study Area

The Niger Delta Basin is located in the Gulf of Guinea on the west coast of Africa, between latitudes 3^0 N and 6^0 N and longitudes 5^0 E and 8^0 E. The Niger delta basin is one of the largest sub aerial basins in Africa. It has a sub aerial area of about 75,000 km^2, a total area of 300,000 km^2, and a sediment fill of 500,000 km^3. The sediment fill has a depth between 9–12 km [10]. Well sections through the Niger Delta generally display three vertical lithostratigraphic subdivisions. These lithostratigraphic units correspond respectively with the Benin Formation (Oligocene-Recent), Agbada Formation (Eocene-Recent) and Akata Formation (Paleocene-Recent) [11].

The Benin formation is Oligocene and younger in age. It is composed of continental flood plain sands and alluvial deposits. It is estimated to be up to 2000 meters thick [10].

The Agbada Formation dates back to Eocene in age [10].

It is the major petroleum-bearing unit in the Niger Delta. The formation consists mostly of shoreface and channel sands with minor shales in the upper part, and alternation of sands and shales in equal proportion in the lower part. The thickness of the formation is over 3,700 metres [11].

The Akata Formation is Paleocene in age. It is composed of thick shales, turbidite sands, and small amounts of silt and clay. It is estimated that the formation is up to 7,000 metres thick [10-11].

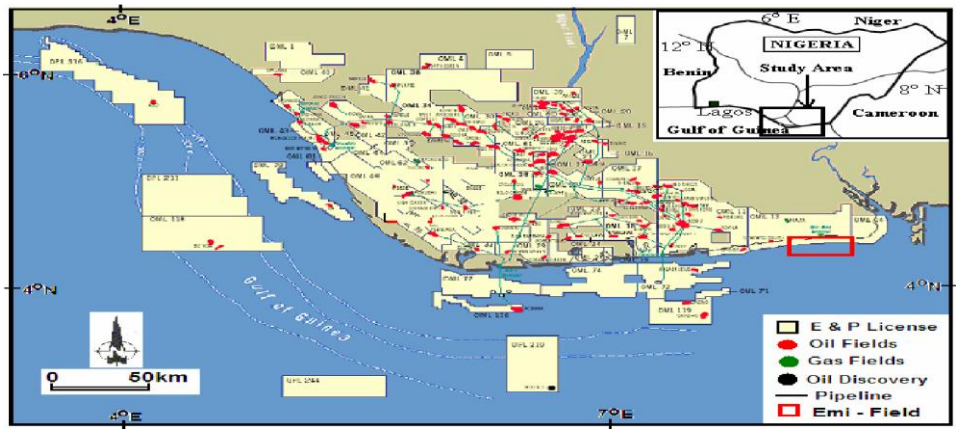

Figure 1: Location of the Field in the Niger Delta [12]

Materials and Methods

Four suits of composite well logs HEK-1, HEK-2, HEK-3, and HEK-4 respectively, obtained from Shell Petroleum Development Company of Nigeria (SPDC) was used for this study. The well logs consists of Sonic,

Gamma ray, resistivity, and neutron and density logs. The sonic and density logs are used to evaluate density, acoustic velocities, and the acoustic impedances from which the lithology discrimination is dependent. The evaluation of these properties is stated below

Determination of Density

Density was gotten from the density log which measures the bulk density of the formation.

Determination of Acoustic Velocity

The sonic log measures the travel time of an elastic wave through the formation from a transmitter to a receiver, which are both mounted on the tool. The acoustic velocity was computed as the reciprocal of the travel time read from the log; given as:

$$V = \frac{1}{\Delta t_{log}} \quad (1)$$

Δt_{log}= travel time from log

Determination of Acoustic Impedance

Acoustic impedance was determined from the formula:

$$Z = \rho \times V \quad (2)$$

Where,

Z= Acoustic impedance, ρ= Density of the formation V= Acoustic velocity of the formation

Discrimination of Lithology

Lithologies of the various depths points for the 4 wells; HEK-1, HEK-2, HEK-3, and HEK-4 would be discriminated using the acoustic impedances values obtained from the ranges of velocity and density values for common matrixes from the table below.

Table 1: Range of Travel Times, Acoustic velocities, bulk densities and Acoustic impedance for common Matrixes in the Niger delta [5, 13-14]

Matrix	Δt (μs/ft)	V (m/s)	ρ (g/cc)	ρ (kg/m^3)	Z (kgm^2s)
Sandstone	55.6 – 51.3	5485.61-5945.42	2.05-2.55	2050-2550	11245500.5-15160821
Limestone	47.6 – 43.5	6407.56-7011.50	2.60-2.80	2600-2800	16659656-19632200
Dolomite	43.5 – 38.5	7011.50-7922.08	2.28-2.90	2280-2900	15986220-22974032
Anhydrite	50.0	6100	2.960	2960	18056000
Halite	66.7	4572.71	2.10-2.40	2100-2400	9602691-10974504
Shale	170 – 60	1794.12-5083.33	2.06-2.66	2060-2660	3695887.2-13521657.8
Bituminous coal	140-100	2178.57-3050	1.200	1200	2614284-3660000

Results and Discussion

The results of the study are presented in tables 2 to 5 and figures 1-12. The figures show the crossplots of the physical parameters of velocity, density and acoustic impedance against depth. These crosplots are discussed below in details.

Cross plot of Depth against Velocity

Figures 1, 4, 7 and 10 are graphical representations of depth against velocity for Wells HEK-1, HEK-2, HEK-3, and HEK-4 respectively. Velocity increases with depth in a normal formation due to compaction. Figures 1, 4, 7 and 10 shows the conventional trend of increasing velocity with increasing depth for we HEK-1,HEK-2,HEK-3, and HEK-4 respectively except the deviation of this trend at some depths, which is as a result of the heterogeneity of formation materials [5].

Cross plot of Depth against Density

Figures 2, 5, 8 and 11 are graphical representations of the plots of depth against density for Wells HEK-1, HEK-2, HEK-3, and HEK-4 respectively. In a normal formation, density increases with depth. Figures 2, 5, 8 and 11 shows the conventional trend of increasing density with increasing depth for wells HEK-1, HEK-2,HEK-3, and

HEK-4 respectively except the deviation of this trend at some depths which could be as a result of conformities in the shale bed [13].

Cross plot of Depth against Acoustic impedance

Figures 3, 6, 9 and 12 are graphical representations of the plots of depth against acoustic impedance for Wells HEK-1, HEK-2, HEK-3, and HEK-4 respectively. In a normal pressured formation, the acoustic impedance always increases with increasing depth, this is because sound wave travels faster in highly compacted medium and the deeper the penetration the more the compaction [14].

Figures 3, 6, 9 and 12 shows the conventional trend of increasing acoustic impedance with increasing depth for wells HEK-1, HEK-2, HEK-3, and HEK-4 respectively except the deviation of this trend at some depths, which could be as a result of under compacted shales that are over pressured [9].

Acoustic Impedance

Acoustic impedance values are presented in the sixth column of Tables 2, 3, 4, 5 for the wells HEK-1, HEK-2, HEK-3, and HEK- 4. The acoustic impedance values for Well HEK-1 ranges from 3544850Kg/m^{2}s - 9514893Kg/m^{2}s, for Well HEK-2 ranges from 14049297Kg/m^{2}s - 6428364Kg/m^{2}s, for Well HEK-3 ranges from 7505579Kg/m^{2}s -7957316Kg/m^{2}s , and for Well HEK- 4 ranges from 3002135Kg/m^{2}s -6833787Kg/m^{2}s.

Table 2: Selected depths, travel times, acoustic velocities, densities, and acoustic impedance of HEK-1

Depth(m)	Δt(μs/ft)	V(m/s)	ρ(g/cc)	ρ(kg/m^3)	Z(kg/m^{2}s)
1222	166.05	1836.71	1.93	1930	3544850
1272	135.8226	2245.41	2.1043	2104.3	4725016
1299	137.2323	2222.23	2.1254	2125.4	4723128
1337	126.1024	2418.65	2.1647	2164.7	5235652
1351	129.9711	2346.67	2.1193	2119.3	4973298
1388	132.7672	2296.955	2.087	2087	4793745
1409	147.5603	2066.68	1.8352	1835.2	3792771
1432	120.2093	2536.99	2.1068	2106.8	5344931
1483	120.2453	2536.38	2.195	2195	5567354
1522	127.7879	2386.625	2.0781	2078.1	4959645
1530	124.22	2455.25	2.1248	2124.8	5216915
1561	120.2477	2536.38	2.1109	2110.9	5354045
1594	127.0948	2399.74	2.1534	2153.4	5167600
1628	117.1429	2603.48	2.236	2236	5821381
1653	123.9535	2460.435	2.1552	2155.2	5302730
1690	126.1178	2418.345	2.1083	2108.3	5098597
1693	124.4568	2450.37	2.134	2134	5229090
1718	113.436	2688.575	2.2182	2218.2	5963797
1755	117.5	2595.55	2.1228	2122.8	5509834
1785	125.2206	2435.425	2.0877	2087.7	5084437
1817	120.3564	2533.94	2.125	2125	5384623
1833	124.7754	2444.27	1.9831	1983.1	4847232
1875	114.6733	2659.6	2.0708	2070.8	5507500
1897	116.1933	2624.83	2.179	2179	5719505
1928	110.7865	2752.93	2.123	2123	5844470
1964	113.6889	2682.475	2.1162	2116.2	5676654
1987	113.8333	2679.12	2.148	2148	5754750
2024	116.0434	2628.185	2.3201	2320.1	6097652
2055	113.8	2680.035	2.1365	2136.5	5725895
2089	103.263	2953.62	2.0868	2086.8	6163614
2124	105.2049	2899.025	2.1708	2170.8	6293203
2147	103.0974	2958.195	2.1885	2188.5	6474010
2174	110.3032	2764.825	2.1554	2155.4	5959304
2199	104.3799	2921.9	2.1221	2122.1	6200564
2242	110.6875	2755.37	2.0375	2037.5	5614066
2267	101.6691	2999.675	2.3507	2350.7	7051336

2299	110.1545	2768.79	2.1769	2176.9	6027379
2324	99.6667	3060.065	2.1822	2182.2	6677674
2350	99.3699	3069.215	2.197	2197	6743065
2383	97.6086	3124.42	2.3369	2336.9	7301457
2420	95.6222	3189.385	2.346	2346	7482297
2443	107.2731	2843.21	2.4152	2415.2	6866921
2489	108.2671	2816.98	2.3168	2316.8	6526379
2509	109.8702	2775.805	2.1004	2100.4	5830301
2542	109.7687	2778.55	2.1	2100	5834955
2582	110.64	2756.59	2.2134	2213.4	6101436
2615	96.9914	3144.55	2.1993	2199.3	6915809
2647	95.9	3180.235	2.245	2245	7139628
2674	93	3279.36	2.3168	2316.8	7597621
2698	101.3022	3010.655	2.323	2323	6993752
2727	94.7	3220.495	2.1707	2170.7	6990728
2759	105.9193	2879.505	2.3414	2341.4	6742073
2790	92.8474	3284.85	2.2295	2229.5	7323573
2812	101.813	2995.405	2.3891	2389.1	7156322
2842	95.7273	3186.03	2.1662	2166.2	6901578
2868	99.9739	3050.61	2.2992	2299.2	7013963
2898	89.8171	3395.565	2.362	2362	8020325
2935	93.8	3251.3	2.4264	2426.4	7888954
2961	102.7075	2969.48	2.4827	2482.7	7372328
2993	88.8	3434.605	2.253	2253	7738165
3026	90.1667	3382.45	2.211	2211	7478597
3049	84.79	3596.865	2.366	2366	8510183
3086	86.759	3515.43	2.282	2282	8022211
3117	89.338	3413.865	2.266	2266	7735818
3139	91.712	3325.415	2.282	2282	7588597
3176	100.97	3020.415	2.362	2362	7134220
3226	88.37	3451.38	2.402	2402	8290215
3235	88.896	3430.945	2.418	2418	8296025
3269	99.745	3057.625	2.335	2335	7139554
3309	95.039	3208.905	2.517	2517	8076814
3333	91.162	3345.545	2.515	2515	8414046
3369	79.92	3816.16	2.447	2447	9338144
3386	81.533	3740.52	2.314	2314	8655563
3417	83.714	3643.225	2.381	2381	8674519
3429	81.759	3730.455	2.358	2358	8796413
3461	74.687	4083.645	2.33	2330	9514893
3477	80.799	3774.68	2.283	2283	8617594
3510	79.299	3846.05	2.287	2287	8795916
3516	77.049	3958.29	2.173	2173	8601364

Table 3: Selected depths, travel times, acoustic velocities, densities, and acoustic impedance of HEK-2

Depth(m)	Δt(μs/ft)	V(m/s)	ρ(g/cc)	ρ(kg/m^3)	Z(kg/m^{2}s)
2048	39.875	7648.79	1.8368	1836.8	14049297
2081	111.5	2735.24	2.1528	2152.8	5888425
2115	107.4375	2838.635	2.1937	2193.7	6227114
2144	105.5	2890.79	2.1976	2197.6	6352800
2185	98.875	3084.465	2.152	2152	6637769
2194	109.4375	2786.785	2.3092	2309.2	6435244
2233	113.0625	2697.42	2.2348	2234.8	6028194
2276	102.25	2982.595	2.1383	2138.3	6377683
2287	110.6875	2755.37	2.351	2351	6477875
2330	101.4375	3006.69	2.2416	2241.6	6739796
2368	107.125	2846.87	2.2583	2258.3	6429087
2402	105.8125	2882.25	2.2659	2265.9	6530890

2421	106.25	2870.355	2.2964	2296.4	6591483
2467	105.8125	2882.25	2.2637	2263.7	6524549
2479	101.6875	2999.37	2.2029	2202.9	6607312
2518	100.5	3034.75	2.2073	2207.3	6698604
2554	104.0625	2930.745	2.38	2380	6975173
2583	98.625	3092.395	2.1595	2159.5	6678027
2612	103.5625	2945.08	2.3446	2344.6	6905035
2639	98.375	3100.325	2.2581	2258.1	7000844
2660	110.9375	2749.27	2.34	2340	6433292
2671	97.9375	3114.05	2.4055	2405.5	7490847
2698	96.375	3164.68	2.3894	2389.4	7561686
2742	93.875	3248.86	2.3475	2347.5	7626699
2755	102.1875	2984.425	2.3878	2387.8	7126210
2759	92.375	3301.625	2.4118	2411.8	7962859
2786	96.8125	3150.345	2.3192	2319.2	7306280
2823	95.0625	3208.295	2.2554	2255.4	7235989
2860	97.625	3124.115	2.3974	2397.4	7489753
2891	90.625	3365.37	2.2192	2219.2	7468429
2921	99.0625	3078.67	2.3825	2382.5	7334931
2927	99.5	3065.25	2.423	2423	7427101
2972	97	3144.245	2.3958	2395.8	7532982
2990	98.3125	3102.155	2.5225	2522.5	7825186
3026	96.25	3168.645	2.3201	2320.1	7351573
3043	94.3125	3233.915	2.1968	2196.8	7104264
3048	94.5625	3225.375	2.3453	2345.3	7564472
3094	94.6875	3221.105	2.3132	2313.2	7451060
3119	96	3176.88	2.3804	2380.4	7562245
3167	93.0625	3277.225	2.335	2335	7652320
3175	93.875	3248.86	2.4151	2415.1	7846322
3185	91.1875	3344.63	2.4052	2405.2	8044504
3201	92	3315.045	2.3948	2394.8	7938870
3256	90.25	3379.4	2.3109	2310.9	7809455
3290	88.75	3436.435	2.4709	2470.9	8491087
3293	75.8125	4022.95	2.235	2235	8991293
3324	60.6875	5025.485	2.2658	2265.8	11386744
3379	92.375	3301.625	2.2785	2278.5	7522753
3391	85.4375	3569.72	2.3911	2391.1	8535557
3437	92	3315.045	2.2347	2234.7	7408131
3467	92.1875	3308.335	2.4269	2426.9	8028998
3502	92.375	3301.625	2.4327	2432.7	8031863
3525	88.5	3446.195	2.3701	2370.1	8167827
3550	86.4375	3528.545	2.3774	2377.4	8388763
3580	87.375	3490.42	2.4571	2457.1	8576311
3611	85.1875	3580.09	2.4325	2432.5	8708569
3637	92.125	3310.47	2.4622	2462.2	8151039
3642	91.4375	3335.48	2.4646	2464.6	8220624
4401	66.5625	4582.015	1.886	1886	8641680
4402	66.625	4577.745	2.1221	2122.1	9714433
4442	77.1875	3951.275	2.3868	2386.8	9430903
4466	100.6875	3028.955	2.4154	2415.4	7316138
4502	102.6875	2970.09	2.4702	2470.2	7336716
4532	113.5625	2685.525	2.4154	2415.4	6486617
4547	123.1875	2475.685	2.5966	2596.6	6428364

Table 4: Selected depths, travel times, acoustic velocities, densities, and acoustic impedance of HEK-3

Depth(m)	Δt(μs/ft)	V(m/s)	ρ(g/cc)	ρ(kg/m^3)	Z(kg/m^{2}s)
1051	73	4177.89	1.7965	1796.5	7505579
1088	142	2147.81	2.0165	2016.5	4331059

1117	143	2132.865	2.042	2042	4355310
1148	135	2259.135	2.1156	2115.6	4779426
1165	129	2364.055	2.1588	2158.8	5103522
1196	142	2147.81	2.0842	2084.2	4476466
1224	142	2147.81	1.9537	1953.7	4196176
1271	125	2440	2.2363	2236.3	5456572
1300	129	2364.055	2.0987	2098.7	4961442
1311	127	2401.57	2.1782	2178.2	5231100
1356	128	2382.66	2.1057	2105.7	5017167
1380	125	2440	2.1341	2134.1	5207204
1409	122	2499.78	2.0976	2097.6	5243539
1443	123	2479.65	2.1104	2110.4	5233053
1488	118	2584.57	2.1798	2179.8	5633846
1500	119	2562.915	2.1656	2165.6	5550249
1550	132	2310.375	2.0994	2099.4	4850401
1583	121	2520.52	2.1196	2119.6	5342494
1595	119	2562.915	2.1789	2178.9	5584335
1623	116	2629.1	2.1528	2152.8	5659926
1656	125	2440	2.1043	2104.3	5134492
1678	120	2541.565	2.2082	2208.2	5612284
1722	114	2675.155	2.1671	2167.1	5797328
1765	109	2798.07	2.1416	2141.6	5992347
1778	111	2747.745	2.1932	2193.2	6026354
1824	110	2772.45	2.1749	2174.9	6029802
1838	116	2629.1	2.3076	2307.6	6066911
1884	105	2904.515	2.1511	2151.1	6247902
1898	92	3315.045	2.0319	2031.9	6735840
1929	103	2960.94	2.2156	2215.6	6560259
1966	118	2584.57	2.3238	2323.8	6006024
1981	98	3112.22	2.3576	2357.6	7337370
2041	103	2960.94	2.2002	2200.2	6514660
2066	106	2877.065	2.1595	2159.5	6213022
2088	111	2747.745	2.2823	2282.3	6271178
2131	106	2877.065	2.1357	2135.7	6144548
2137	104	2932.575	2.21	2210	6480991
2164	107	2850.225	2.1857	2185.7	6229737
2211	106	2877.065	2.3361	2336.1	6721112
2253	100	3050	2.2232	2223.2	6780760
2284	102	2989.915	2.1442	2144.2	6410976
2300	100	3050	2.1646	2164.6	6602030
2338	104	2932.575	2.1469	2146.9	6295945
2353	103	2960.94	2.1752	2175.2	6440637
2405	104	2932.575	2.3669	2366.9	6941112
2418	98	3112.22	2.1558	2155.8	6709324
2455	104	2932.575	2.2048	2204.8	6465741
2494	104	2932.575	2.124	2124	6228789
2525	105	2904.515	2.1281	2128.1	6181098
2534	111	2747.745	2.2976	2297.6	6313219
2580	102	2989.915	2.2977	2297.7	6869928
2620	100	3050	2.1698	2169.8	6617890
2629	109	2798.07	2.2026	2202.6	6163029
2662	104	2932.575	2.3792	2379.2	6977182
2700	93	3279.36	2.3024	2302.4	7550398
2722	98	3112.22	2.3145	2314.5	7203233
2768	90	3388.855	2.4125	2412.5	8175613
2779	109	2798.07	2.3347	2334.7	6532654
2830	89	3426.675	2.1899	2189.9	7504076
2840	91	3351.645	2.4319	2431.9	8150865

2875	104	2932.575	2.3047	2304.7	6758706
2908	89	3426.675	2.1593	2159.3	7399219
2950	89	3426.675	2.3169	2316.9	7939263
2968	95	3210.43	2.2421	2242.1	7198105
3001	94	3244.59	2.1912	2191.2	7109546
3018	86.2	3538	2.2491	2249.1	7957316

Table 5: Selected depths, travel times, acoustic velocities, densities, and acoustic impedance of HEK-4

Depth(m)	Δt(μs/ft)	V(m/s)	ρ(g/cc)	ρ(kg/m^3)	Z(kg/m^{2}s)
1891	170.8761	1784.86	1.682	1682	3002135
1941	118.373	2576.335	2.043	2043	5263452
1971	122.1384	2497.035	2.2432	2243.2	5601349
1997	117.2787	2600.43	2.2185	2218.5	5769054
2028	106.6919	2858.46	2.1608	2160.8	6176560
2070	112.0637	2721.515	2.217	2217	6033599
2073	104.9746	2905.43	2.1276	2127.6	6181593
2124	109.668	2780.99	2.1714	2171.4	6038642
2149	109.94	2773.975	2.2958	2295.8	6368492
2176	110.5533	2758.725	2.3393	2339.3	6453485
2204	104.3227	2923.425	2.2516	2251.6	6582384
2242	106.2115	2871.575	2.2863	2286.3	6565282
2281	106.6783	2858.765	2.1591	2159.1	6172360
2290	102.6993	2969.785	2.403	2403	7136393
2331	105.0604	2902.99	2.3811	2381.1	6912309
2370	96.3044	3166.815	2.2386	2238.6	7089232
2394	95.5753	3190.91	2.2599	2259.9	7211138
2422	85.4814	3567.89	2.2027	2202.7	7858991
2462	100.5389	3033.53	2.3439	2343.9	7110291
2498	97.3356	3133.265	2.3015	2301.5	7211209
2518	100.725	3028.04	2.365	2365	7161315
2545	93.7362	3253.74	2.3577	2357.7	7671343
2570	98.6854	3090.565	2.3787	2378.7	7351527
2593	97.5344	3126.86	2.3562	2356.2	7367508
2645	91.0753	3348.595	2.3424	2342.4	7843749
2676	89.2373	3417.83	2.3216	2321.6	7934834
2702	96.2045	3170.17	2.4141	2414.1	7653107
2739	91.2531	3342.19	2.3612	2361.2	7891579
2757	93.1286	3274.785	2.3262	2326.2	7617805
2781	92.7055	3289.73	2.3779	2377.9	7822649
2796	104.2726	2924.95	2.677	2677	7830091
2797	106.8576	2854.19	2.3943	2394.3	6833787

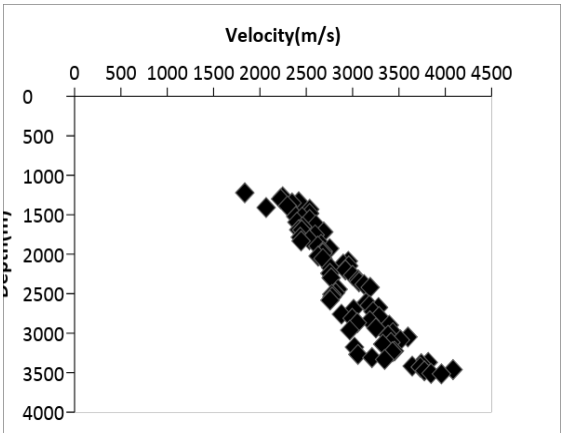

Figure 1: Cross plot of Depth against Velocity for HEK-1

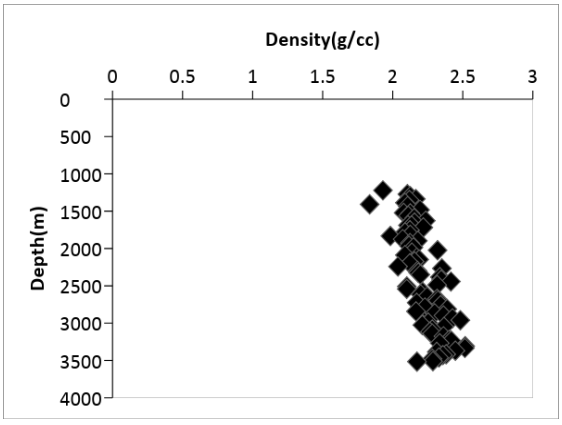

Figure 2: Cross plot of Depth against Density for HEK-1

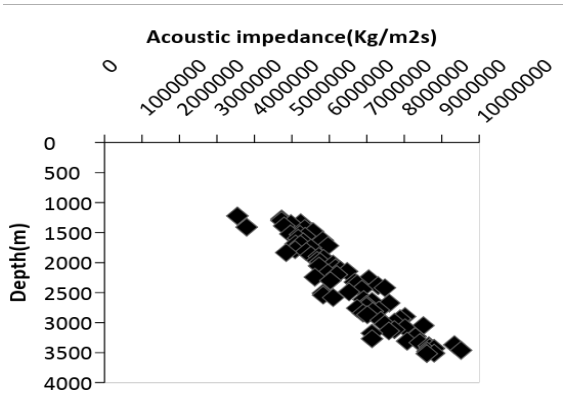

Figure 3:Cross plot of Depth against Acoustic impedance for HEK-1

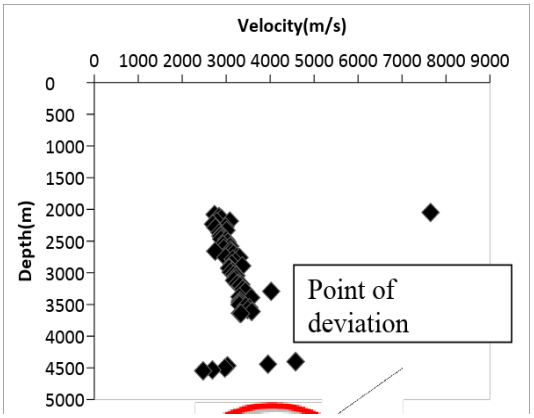

Figure 4: Cross plot of Depth against Velocity for HEK-2

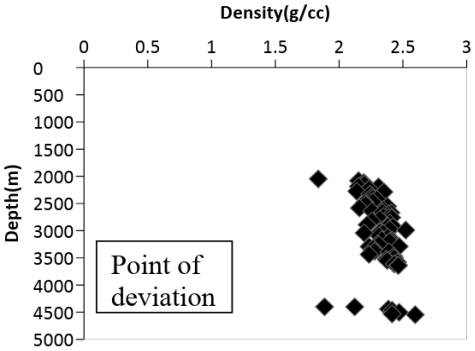

Figure 5: Cross plot of Depth against Density for HEK-2

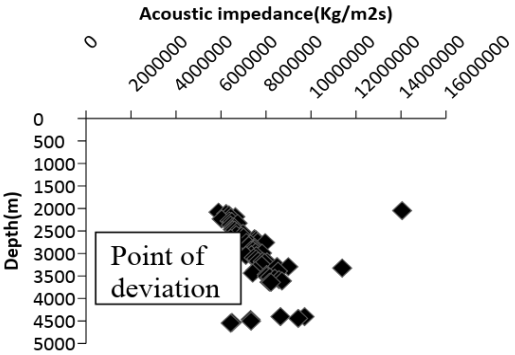

Figure 6: Cross plot of Depth against Acoustic impedance for HEK-2

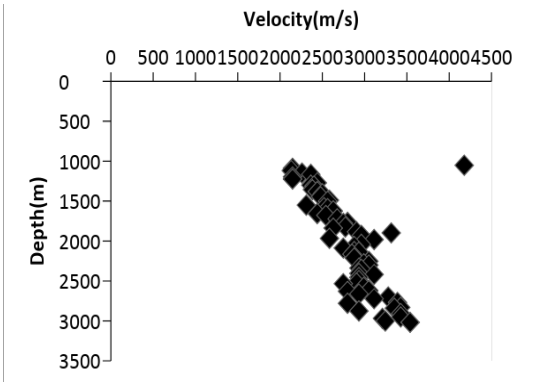

Figure 7: Cross plot of Depth against Velocity for HEK-3

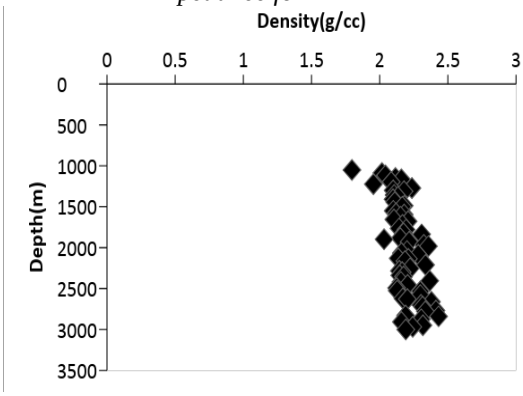

Figure 8: Cross plot of Depth against Density for HEK-3

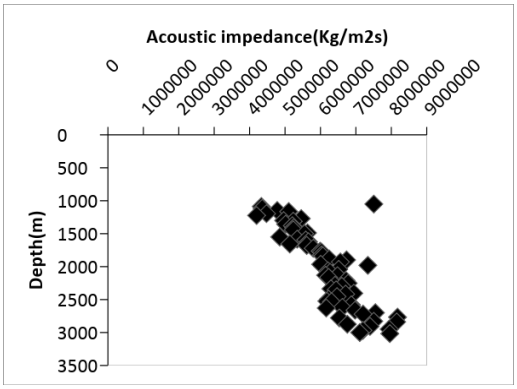

Figure 9: Cross plot of Depth against Acoustic impedance for HEK-3

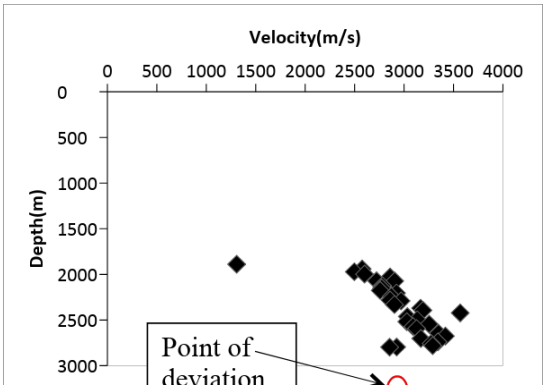

Figure 10: Cross plot of Depth against Velocity for HEK-4

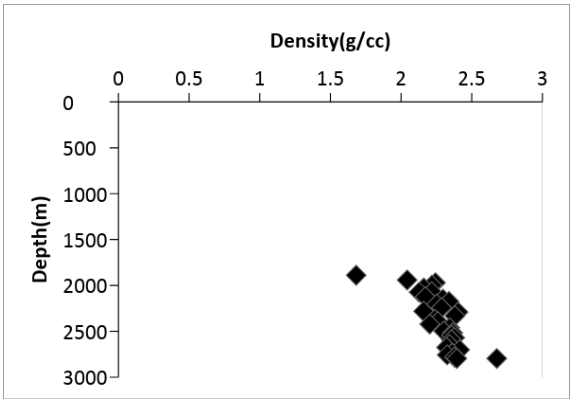

Figure 11: Cross plot of Depth against Density for HEK-4

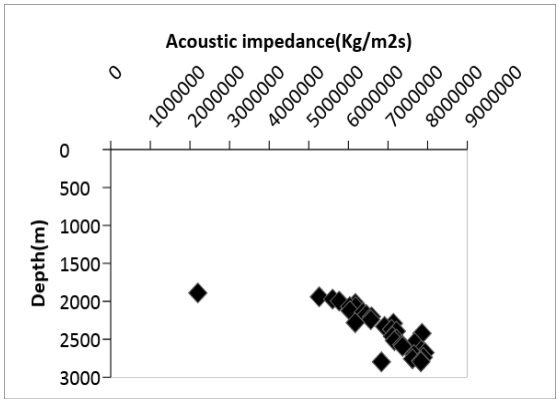

Figure 12: Cross plot of Depth against Acoustic impedance for HEK-4

Conclusion

The analysis and interpretations of the data obtained and computed values affirmed the conventional trend of increasing velocity with depth, increasing density with depth, and increasing acoustic impedance with depth in the Niger Delta, with some variations in the trend attributed to the heterogeneity in the formation material due to velocity, conformities in the shale bed due to density, and under compacted shales that are over pressured due to acoustic impedance. The acoustic impedance values from Tables 2, 3, 4, and 5 ranges from 3002135Kg/m^{2}s-14049297Kg/m^{2}s. Taking Table 1 as the reference, HEK-1 shows a shale formation, HEK-2 indicates a shale formation with variations at depths 2048m and 3324m of acoustic impedance 14049297Kg/m^{2}s and 11386744Kg/m^{2}s respectively which are possible indications of sandstone, HEK-3 shows a shale formation, and HEK-4 also shows a shale formation. The result generally shows a shaly formation across the wells. Hence, confirming the established lithology of the Niger Delta. The results of this study can aid in carrying out accurate petrophysical calculations of porosity, water saturation and permeability.

Acknowledgements

The authors are grateful to Shell Petroleum Development Company of Nigeria (SPDC) Port Harcourt Nigeria for the release of the academic data for the purpose of this study

References

[1]. Bello, R., Igwenagu, C. L., & Onifade, Y. (2015). Cross plotting of Rock Properties for Fluid and Lithology Discrimination using Well Data in a Niger Delta Oil Field. *Journal of Applied Sciences and Environmental Management, 19*(3), 539-546.

[2]. Plummer, C. C., & McGeary, D. (1993). *Physical Geology* (6th Edition ed.). England: Brown publishers.

[3]. Tamunobereton-ari, I., Omubo-Pepple,V.B.,Uko, E.D. (2011). Determination of the Variability of Seismic Velocity with Lithology in the South-Western Part of the Niger Delta Basin of Nigeria Using Well Logs. *Journal of Basic and Applied Scientific Research, 1*(7), 700-705.

[4]. Uko, E. D., Amakiri, A. R. C., & Alagoa, K. D. (2002). Effects of Lithology on Geothermal Gradient in the South-east Niger Delta. *Global Journal of Pure and Applied Science, 9*(3), 325 – 337.

[5]. Tamunobereton-ari, I., Uko, E. D., & Omubo-Pepple, V. B. (2013). Estimation of lithological and mineralogical contents of rocks from Matrix density in part of Niger Delta Basin Nigeria, using Well-log Data. *Journal of Emerging Trends in Engineering and Applied Sciences, 4*(6), 828-836.

[6]. Petrowiki. (2015). Lithology and rock type determination Retrieved Febuary, 2016, from petrowiki.org/lithology and rock type determination#.VugDaTNw3TY.

[7]. Sheriff, R. E. (Ed.) (1991) (3rd Edition ed.). USA: Society of Exploration Geophysicists.

[8]. Telford, W. M., Geldart, L. P., & Sheriff, R. E. (1990). *Applied Geophysics* (2nd Edition ed.). New York: Cambridge University Press.

[9]. Horsfall, O. I., Omubo-Pepple, V. B., & Tamunobereton-ari, I. (2014). Estimation of Shear Wave Velocity for Lithological Variation in the North-Western Part of the Niger Delta Basin of Nigeria. *American Journal of Scientific and Industrial Research*, *5*(1), 13-22.

[10]. Wikipedia. (2016). Niger Delta Basin (Geology) Retrieved 13th May, 2016, from https://en.wikipedia.org/wiki/Niger_Delta_Basin_%28geology%29

[11]. Ajaegwu, N. E., Odoh, B. I., Akpunonu, E. O., Obiadi, I. I., & Anakwuba, E. K. (2012). Late Miocene to Early Pliocene Palynostratigraphy and Palaeoenvironments of ANE-1 Well, Eastern Niger Delta, Nigeria. *Journal of Mining and Geology*, *48*(1), 31–43.

[12]. Nton, M. E. & Esan, T. B. (2010). Sequence Stratigraphy of EMI Fields, Offshore Eastern Niger Delta, Nigeria. *European Journal of Scientific Research*, 44(1), 115 – 132.

[13]. Glover, P. (2013). The formation density log. *Petrophysical Msc Course note*, 121-138.

[14]. Glover, P. (2016). Sonic (Acoustic) log. *Petrophysical Msc course notes*, 172-197.